Analytica Chimica Acta xxx (2015) 1–8

Contents lists available at ScienceDirect

Analytica Chimica Acta

journal homepage: www.elsevier.com/locate/aca

Coupling a universal DNA circuit with graphene sheets/polyaniline/AuNPs nanocomposites for the detection of BCR/ABL fusion gene

Xueping Chen [a], Li Wang [a, b], Shangchun Sheng [c], Teng Wang [a], Juan Yang [a], Guoming Xie [a, **], Wenli Feng [a, *]

[a] Key Laboratory of Laboratory Medical Diagnostics of Education, Department of Laboratory Medicine, Chongqing Medical University, Chongqing, 400016, PR China
[b] Department of Medical Laboratory, Chongqing Emergency Medical Center (Chongqing The Fourth Hospital), Chongqing, 400016, PR China
[c] The No.2 Peoples' Hospital of Yibin, Sichuan, 644000, PR China

HIGHLIGHTS

- A transducer hairpin was designed to improve the versatility of DNA circuit.
- GS/PANI/AuNPs were introduced to the DNA circuit for further signal amplification.
- The established biosensor displayed high sensitivity and good specificity.

GRAPHICAL ABSTRACT

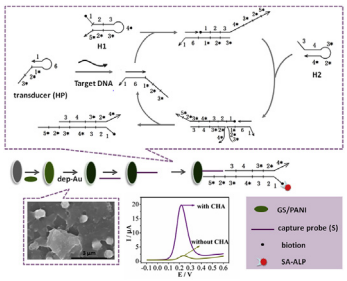

ARTICLE INFO

Article history:
Received 12 February 2015
Received in revised form
7 June 2015
Accepted 30 June 2015
Available online xxx

Keywords:
BCR/ABL fusion gene
Universal DNA circuit
Catalyzed hairpin assembly
Transducer hairpin
Electrochemical DNA biosensor

ABSTRACT

This article described a novel method by coupling a universal DNA circuit with graphene sheets/polyaniline/AuNPs nanocomposites (GS/PANI/AuNPs) for highly sensitive and specific detection of BCR/ABL fusion gene (bcr/abl) in chronic myeloid leukemia (CML). DNA circuit known as catalyzed hairpin assembly (CHA) is enzyme-free and can be simply operated to achieve exponential amplification, which has been widely employed in biosensing. However, application of CHA has been hindered by the need of specially redesigned sequences for each single-stranded DNA input. Herein, a transducer hairpin (HP) was designed to obtain a universal DNA circuit with favorable signal-to-background ratio. To further improve signal amplification, GS/PANI/AuNPs with excellent conductivity and enlarged effective area were introduced into this DNA circuit. Consequently, by combining the advantages of CHA and GS/PANI/AuNPs, bcr/abl could be detected in a linear range from 10 pM to 20 nM with a detection limit of 1.05 pM. Moreover, this protocol showed excellent specificity, good stability and was successfully applied for the detection of real sample, which demonstrated its great potential in clinical application.

* Corresponding author. Key Laboratory of Laboratory Medical Diagnostics of Education, Department of Laboratory Medicine, Chongqing Medical University, No. 1 Yi Xue Yuan Road, Chongqing, 400016, PR China.
** Corresponding author. Key Laboratory of Laboratory Medical Diagnostics of Education, Department of Laboratory Medicine, Chongqing Medical University, No. 1 Yi Xue Yuan Road, Chongqing, 400016, PR China.
E-mail addresses: guomingxie@cqmu.edu.cn (G. Xie), fengwlcqmu@sina.com (W. Feng).

http://dx.doi.org/10.1016/j.aca.2015.06.050
0003-2670/

1. Introduction

Chronic myeloid leukemia (CML) is a myeloproliferative disease characterized by reciprocal translocation t (9; 22) (q34; q11) which lead to the generation of BCR/ABL fusion gene (bcr/abl) [1]. Thus, bcr/abl has been an important biomarker for early diagnosis, regular molecular assay, and therapeutic drug monitoring of CML [2]. Currently, mostly used methods for the detection of bcr/abl are real-time quantitative polymerase chain reaction, flow cytometry, fluorescence in situ hybridization, and chromosome analysis. Despite their excellent performances, these approaches are yet to be adaptable for point-of-care use. The major barriers involve their requirements for special laboratory skills and costly instrumentations [3]. In addition, measurement of bcr/abl for diagnosis of minimal residual disease (MRD) is still a great challenge due to the sensitivity limit of current methods [4]. Therefore, easy-to-use, cost-effective, and highly sensitive methods for bcr/abl detection are still greatly needed.

The inherent superiorities of electrochemical biosensor, such as good portability, low cost, and high sensitivity, make it considerably attractive for target detection [5,6]. Up to now, various electrochemical DNA biosensors based on signal amplification strategies for sensitive detection of target DNA (C1) have been reported, including polymerase chain reaction [7], rolling circle amplification [8], endonuclease-assisted approach [9] and so on. However, most of these methods require protein enzymes which are costly and sensitive to experimental conditions. Recently, signal amplification strategies which are independent of protein enzymes show great potential in point-of-care diagnosis [10,11]. Of particular interest is a programming DNA circuit known as catalyzed hairpin assembly (CHA). CHA is an enzyme-free and cost-effective amplification method which overcomes the disadvantages of enzyme-based strategies [12,13]. CHA is developed from DNA nanostructure organization and based on toehold-mediated strand displacement. Due to the excellent properties of CHA, it has yielded increasing real-life applications in diagnostics, nanotechnology, and synthetic biology [14–16]. In detail, CHA can achieve exponential or polynomial amplification, which has been widely employed for analysis of protein [17], nucleic acid [18], and small molecule [19]. However, most studies of CHA have focused on the design of sequences for different targets, which are highly rely on specially redesigned sequences for different kinds of single-stranded DNA input. Besides, ideal catalyst strand for CHA is divided into three domains with 8 nt of each domain. So target DNA directly used as catalyst strand sequence for CHA is required to be about 24 nt, which limits the versatility of CHA. Furthermore, signal leakage caused by non-specific background has also become a problem [20]. Thus, to wider the application of CHA, a universal DNA circuit with favorable signal-to-background ratio is expected.

Recently, a number of electrochemical approaches for testing bcr/abl have been evolved. For instance, abbhairpin DNA probe based approach with a detection limit of 5.3 nM [21] and nanogold-modified poly-eriochrome black T film based route with a detection limit of 10 pM [22] are reported. These methods are sensitivity limited without effective signal amplification strategy. More recently, polymerase coupling with quantum dot tagging is used for ultrasensitive detection of bcr/abl [23]. But this method is enzyme dependent with complex procedures. Over the last decades, nanomaterials have been explored intensively in biosensing applications, owing to their unique chemical and physical properties [24]. Nanocomposites which consist of graphene sheet (GS), polyaniline (PANI), or AuNPs have drawn particular attention due to their excellent conductivity, enlarged effective area and good biocompatibility [25–27]. However, GS, PANI and AuNPs nanocomposites are usually synthesized by multi-step processes which are time-cosuming. Facile and powerful amplification methods are required.

Herein, we developed a novel sensing strategy by combining a universal DNA circuit with simply synthesized GS/PANI/AuNPs for highly sensitive and specific detection of bcr/abl. In detail, a transducer hairpin (HP) was designed for CHA to enable reuse of the DNA circuit for different inputs DNA. The NUPACK package [28] was used to analyze the sequences of each probe to improve signal and degrade background. By optimizing sequences and concentration of HP, signal-to-background ratio could be improved. In addition, GS/PANI/AuNPs with excellent conductivity and enhanced effective area were coupled with CHA for further signal amplification, which might contribute to highly sensitive detection of bcr/abl. By combing the advantages of CHA and GS/PANI/AuNPs, this proposed protocol exhibited excellent analytical performance toward bcr/abl. And this method was successfully applied for real sample from CML patients with satisfactory results, which demonstrated its great potential in clinical application.

2. Experimental

2.1. Reagents and materials

Oligonucleotides were ordered from Shanghai Sangon Biotechnology Co. Ltd. (Shanghai, China). Oligonucleotides sequences are listed in Table S1. All DNA strands were stored in 1 × TE (10 mM Tris–HCl, 1 mM EDTA, pH 7.5) at 20 °C. Graphene sheets (GS) were purchased from Pioneer Nanotechnology Co. Ltd. (Nanjing, China). Aniline (99%+) were purchased from Adamas Reagent Co. Ltd. (Brussels, Switzerland). The chloroauric acid ($HAuCl_4$), streptavidin-alkaline phosphatase (SA-ALP), 1-naphthyl phosphate (1-NP, 99%), 6-mercapto-1-hexanol (MCH), and bovine serum albumin (BSA, 99%) were purchased from Sigma Chemical Co. Ltd. (St. Louis, USA). The primers used for PCR were purchased from BGI Inc. (Beijing, China) and their sequences were showed in Table S1. DL2000 DNA Marker, DL500 DNA Marker, Premix Taq Version 2.0, and agarose were purchased from Takara Co. Ltd. (Dalian, China). All chemicals were of analytical grade and used as received unless other indicated. Deionized water was obtained from a Millipore-Q water purification system (≥18 MΩ, Milli-Q, Millipore) and used in all runs. Tris–HCl buffer (20 mM Tris, 0.1 M NaCl, 5 mM $MgCl_2$, 0.005% Tween-20, pH 7.4) was used as washing buffer. 1 × TNaK buffer (20 mM Tris, 140 mM NaCl, 5 mM KCl, pH 7.4) was used as DNA hybridization buffer. DEA buffer (0.1 M diethanol amine, 1 M $MgCl_2$ and 10 mM KCl, pH 9.62) was used as working buffer for electrochemical detection.

2.2. Apparatus

Cyclic voltammetry (CV), electrochemical impedance spectroscopy (EIS) and differential pulse voltammetry (DPV) were performed with a electrochemical workstation (CHI-660D, Shanghai Chenhua Instruments Co. Ltd., China) using a conventional three-electrode system with an Ag/AgCl (1 M KCl) electrode as the reference electrode, a Pt wire as the counter electrode, and a modified glassy carbon electrode (GCE) as the working electrode. The synthesized nanocomposites were characterized by a field emission scanning electron microscope (SEM) system (FEI Nova-400, USA) and an atomic force microscope (AFM) (NanoWizard II, JPK Instruments Inc., Germany). Energy dispersive X-ray (EDX) spectra of GS/PANI/AuNPs were analyzed by a scanning electron microscope (VEGA3 SB, TESCAN Co. Ltd., Czech Republic).

Please cite this article in press as: X. Chen, et al., Coupling a universal DNA circuit with graphene sheets/polyaniline/AuNPs nanocomposites for the detection of BCR/ABL fusion gene, Analytica Chimica Acta (2015), http://dx.doi.org/10.1016/j.aca.2015.06.050

2.3. Fabrication of the DNA biosensor

Prior the experiment, GS/PANI was prepared according to previous method with a slight modification [29], which was illustrated in supporting information. Firstly, GCE was polished to a mirror face with 0.3 and 0.5 μm alumina powders. Then, GCE was ultrasonically washed in deionized water, ethanol, and deionized water, orderly. Next, 5 μL of prepared GS/PANI solution was deposited on the precleaned GCE surface and dried at room temperature (RT). The modified electrode was labeled as GS/PANI/GCE. Then electrodeposition of AuNPs (dep-Au) was performed in 1% $HAuCl_4$ solution by CV at a potential from 0.2 to 0.6 V for 50 s [30], the obtained electrode was noted as GS/PANI/AuNPs/GCE. For immobilization, 10 μL of 1 μM thiolated capture probe (S) was dropped onto the surface of GS/PANI/AuNPs/GCE and incubated overnight at 4 °C. After washing with buffer, the electrode was immersed in 1 mM MCH for 1 h, followed by treating with 1% BSA for 30 min to prevent non-specific adsorption and block the remaining bare area. After washing with buffer, the finally obtained biosensor was stored at 4 °C for future use.

2.4. Catalyzed hairpin assembly and electrochemical measurement

Prior experiments, HP, hairpin (H1) and hairpin (H2) were separately heated in 1 × TNaK buffer at 95 °C water bath for 5 min, followed by slowly cool to RT over the course of 90 min to avoid unwanted structure [31]. Firstly, different concentrations of target DNA (20 μL, 6 × final concentration) was mixed with HP (20 μL, 6 × final concentration), and incubated at 37 °C for 30 min, followed with addition of H1 (40 μL, 3 × final concentration) and H2 (40 μL, 3 × final concentration). The final concentration of HP, H1, and H2 was 20 nM, 50 nM and 50 nM, respectively. Secondly, the mixtures were incubated for 60 min at 37 °C, which led to the formation of H1:H2 and the recycle of C1:HP. Thirdly, 10 μL of the above mixtures were placed on prepared electrode and incubated for another 60 min at 37 °C. As a result, S:H1:H2 complex were formed, and then the electrode was roughly rinsed with DEA buffer to remove unbound probes. Fourthly, 10 μL of DEA buffer (0.5 μg mL^{-1} SA-ALP, 10 mg mL^{-1} BSA) was cast onto the electrode surface and incubated for 30 min at 37 °C, followed by washing with DEA buffer containing 0.05% Tween-20. Finally, DPV was performed in DEA buffer containing 1 mg mL^{-1} 1-NP with modulation time of 0.05 s, interval time of 0.017 s, step potential of 5 mV, modulation amplitude of 70 mV and potential scan from −0.1–0.6 V.

2.5. Preparation of real samples

K562 cells and real samples from the bone marrow cells were gifted by the First Affiliated Hospital, Chongqing Medical University. PCR products of BCR/ABL fusion gene and β-actin were obtained according to our previous method [32]. The PCR products were analyzed by electrophoresis on 2% agarose gel. Before use, PCR products were denatured at 95 °C for 5 min and chilled on ice.

3. Results and discussion

3.1. Principle of this protocol

The principle of this protocol was depicted in Scheme 1. Briefly, CHA reaction mixtures containing C1, HP, biotin labeled H1, and H2 were placed on the prepared GCE surface. H1:H2 duplex was the product of CHA which hybridized with S and bound to the electrode surface, followed with covalent binding of SA-ALP and biotin labeled H1 via biotin-avidin system. Current signal was gained using 1-NP as the enzymatic substrate.

The sequences of H1 and H2 were designed according to previous reports [33] with a slight modification. To make a universal DNA circuit, we designed HP as the transducer and S as the capture probe. Sequences of each probe were rationally designed to improve signal and degrade background. NUPACK was used to analyze structures of these hairpins (Fig S1). CHA procedure was shown in Scheme 1. In the absence of C1, domain 1* of HP was occluded by its domain 1 (10 nt) to form stable hairpin structured. HP barely hybridized with H1 when its toehold (domain 1*) was occupied. And H1 could hardly bind to S with only 6 nt (domain 5*) complementary to S. Thus the background could be degraded. In the presence of C1, C1 bound to the loop of HP and unfolded HP, which spontaneously formed a HP:C1 duplex. Then, the exposed domain 1* of HP became an active toehold, which triggered the hybridization between H1 and HP:C1 duplex. After branch migration, hairpin H1 was unfolded and its domain 3* was exposed. Domain 3* of H1 as a toehold then bound to domain 3 of H2, and HP:C1 duplex was displaced by H2 via toehold-mediated displacement. As a result, HP:C1 was relieved and available to trigger another cycle. Meanwhile, domain 2* of H1 with another 8 nt complementary to S was exposed which allowed the stable formation of S:H1:H2 complex on the modified electrode surface.

3.2. Characterization of GS/PANI/AuNPs

The nanocomposites were characterized by SEM and EDX. Immobilization of S was analyzed by AFM. SEM image of GS/PANI was shown in Fig. 1A. PANI with typical branch structure was homogeneously surrounded around GS. SEM image of GS/PANI/AuNPs (Scheme 1) exhibited that AuNPs bound to the GS/PANI matrix surface without any conglomeration. This was because that PANI provided a steric barrier against the aggregation AuNPs [34]. Furthermore, chitosan (CS) could bond these AuNPs via hydroxyl groups when the nanocomposites were re-dispersed in CS, which also contributed to the solubility and stability of AuNPs [35]. According to EDX spectrum (Fig. 1B), GS/PANI/AuNPs were composed of mainly Au and large amounts of C and N, demonstrating that constituent of GS/PANI/AuNPs were in accordance with GS, PANI and AuNPs. As shown in AFM images, GS/PANI/AuNPs/GCE (Fig. 1C) presented a rough and granular appearance. However, S/GS/PANI/AuNPs/GCE (Fig. 1D) displayed a more aggregated image due to the addition of S, which confirmed the successful immobilization of S.

3.3. Electrochemical characterization

The stepwise reactions on the surface of GCE were characterized by EIS. Fig. 2 showed the nyquist plots of different modified electrodes in 5 mM $Fe(CN)_6^{3-/4-}$ solution. The semicircle diameter corresponded to the charge transfer resistance (R_{ct}) on the electrode. Compared with bare GCE (curve a), the GS/PANI/AuNPs modified GCE (curve b) revealed an almost straight line, implying its R_{ct} decreased due to the superior conductivity of GS/PANI/AuNPs. After immobilization of S, R_{ct} increased (curve c) because of the negative charged phosphoric acid backbones of DNA probe which was able to hinder the electron transmission. The R_{ct} increased significantly after the modified electrode was blocked with MCH and BSA (curve d and e). With the addition of CHA reaction mixtures, higher R_{ct} was obtained (curve f). This was mainly due to the formation of dsDNA with much more negatively charged phosphoric acid backbones. Finally, the R_{ct} increased continuatively (curve g) when the SA-ALP attached on the electrode surface, indicating the successful binding of SA-ALP which retard the electron transfer.

EIS and CV were employed to analyze the electron transfer

Please cite this article in press as: X. Chen, et al., Coupling a universal DNA circuit with graphene sheets/polyaniline/AuNPs nanocomposites for the detection of BCR/ABL fusion gene, Analytica Chimica Acta (2015), http://dx.doi.org/10.1016/j.aca.2015.06.050

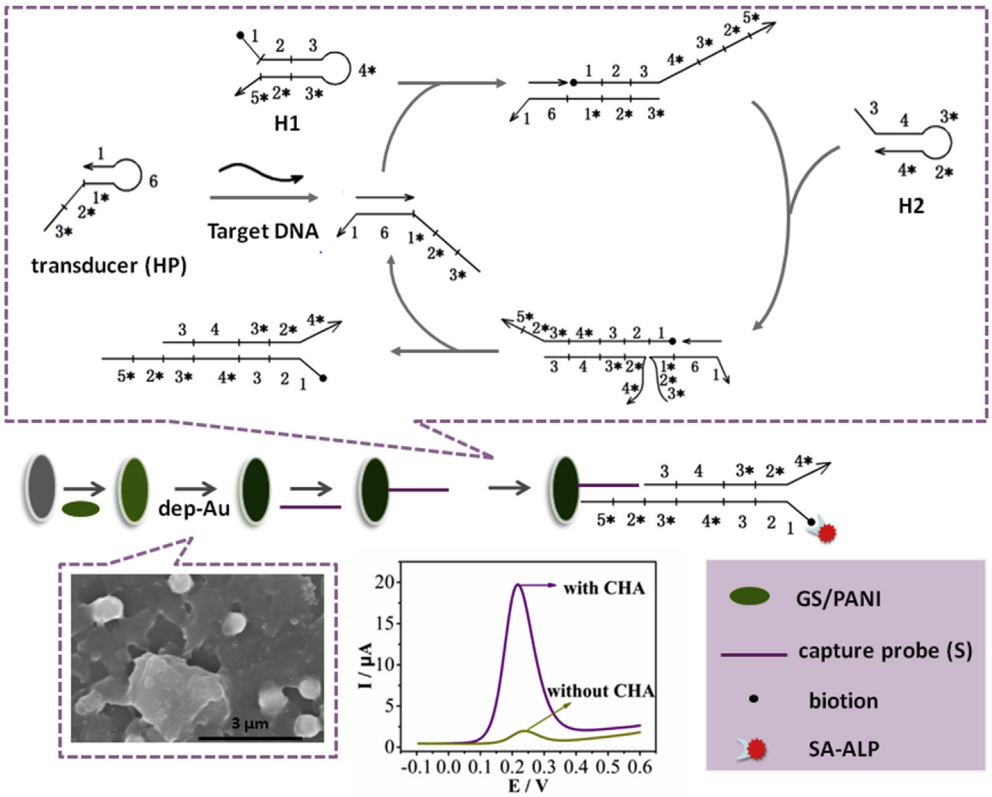

Scheme 1. Schematic illustration of the sensing strategy for the detection of target DNA based on a universal DNA circuit and graphene sheets/polyaniline/AuNPs.

capability of different nanocomposites (Inset A and B in Fig. 2). GS/PANI/AuNPs/GCE exhibited smaller R_{ct} and higher peak current compared with GS/GCE, PANI/GCE, or GS/PANI/GCE, which was due to its excellent conductivity and enlarged accessible surface area. The signal amplification capacity of GS/PANI/AuNPs was further confirmed by DPV (Fig. S2). DPV results were consisted with that of EIS and CV.

3.4. Feasibility of the universal DNA circuit

DPV was used to demonstrate feasibility of the DNA circuit. As shown in Fig. 3A, in the absence of C1, reaction mixtures containing H1 and HP did not elicit an observable current (curve a), as well as mixtures containing H1, HP and H2 (curve b). These results indicated the low background of CHA. The rationally designed hairpins which greatly avoid their unwanted secondary structures may contribute to the low background. In detail, long stem of each probes enabled them to be in stable hairpin structures in the absence of C1, which could degrade background. When C1 appeared, the signal peak current was only 1.369 μA (curve c) in the absence of H2. With addition of H2, the signal peak current increased to 19.73 μA (curve d) which suggested a roughly 10-fold amplification by the DNA circuit. This was because CHA could lead to the recycle of catalyzed strand. The toehold of each hairpin assisted to unfold the hairpin structure in the presence of C1, resulting in the signal amplification.

Agarose gel electrophoresis was further used to identify the performance of CHA based on toehold-mediated strand displacement. In Fig. 3B, the corresponding bands of H1 (lane 1), H2 (lane 2), C1 (lane 3), and HP (lane 4) were figured out. Comparing lane 4 and 5, new band emerged after addition of C1which indicated the formation of C1:HP. The mixtures of C1, HP, and H1 showed a weak band at the position HP, and a new bright band with lower mobility (lane 7) compared with lane 5. It demonstrated the hybridization between C1:HP duplex and H1. Through comparing the other lanes with lane 9, we drew a conclusion that H2 replaced C1:HP on H1, so brighter bands were observed due to the formation of C1:HP and H1:H2. Because C1:HP and H1:H2 possessed similar base number, the bands of them were too close to be separated and brighter than other bands.

3.5. Optimization of experimental conditions

Experimental conditions were the key factors that influenced analytical performances of the biosensor, such as probe concentration and incubation time. The ideal system should give a significant increase of signal upon the addition of C1, while a relative low background in the absence of C1. To improve signal-to-background ratio (S/B), effects of the length of HP stem, concentration of HP, concentration of H2, and assembly time for CHA were investigated by DPV. As illustrated in Fig. 4A, signal and background decreased along with increasing length of HP stem. Because longer stem was in favor of stable hairpin structure thus degrade background, while it was against the hybridization between HP and C1 and led to relative lower signal. For the sake of S/B, 10 nt was chosen as the stem length of HP. As shown in Fig. 4B, signal increased with HP concentration in the range from 5 to 40 nM, and the background also increased due to spare HP. Therefore, 20 nM was used for the following experiments considering S/B. Fig. 4C presented the effect of the H2 concentration. Signal continuously increased with H2 concentration ranging from 10 to 90 nM. This was because more HP:C1 duplex complex could be displaced and recycled for signal amplification. However, obvious background was gained with higher H2 concentration. Therefore, 50 nM had been chosen as the optimized condition. The sensing process was also influenced by the assembly time of CHA. As shown in Fig. 4D, signal and

Please cite this article in press as: X. Chen, et al., Coupling a universal DNA circuit with graphene sheets/polyaniline/AuNPs nanocomposites for the detection of BCR/ABL fusion gene, Analytica Chimica Acta (2015), http://dx.doi.org/10.1016/j.aca.2015.06.050

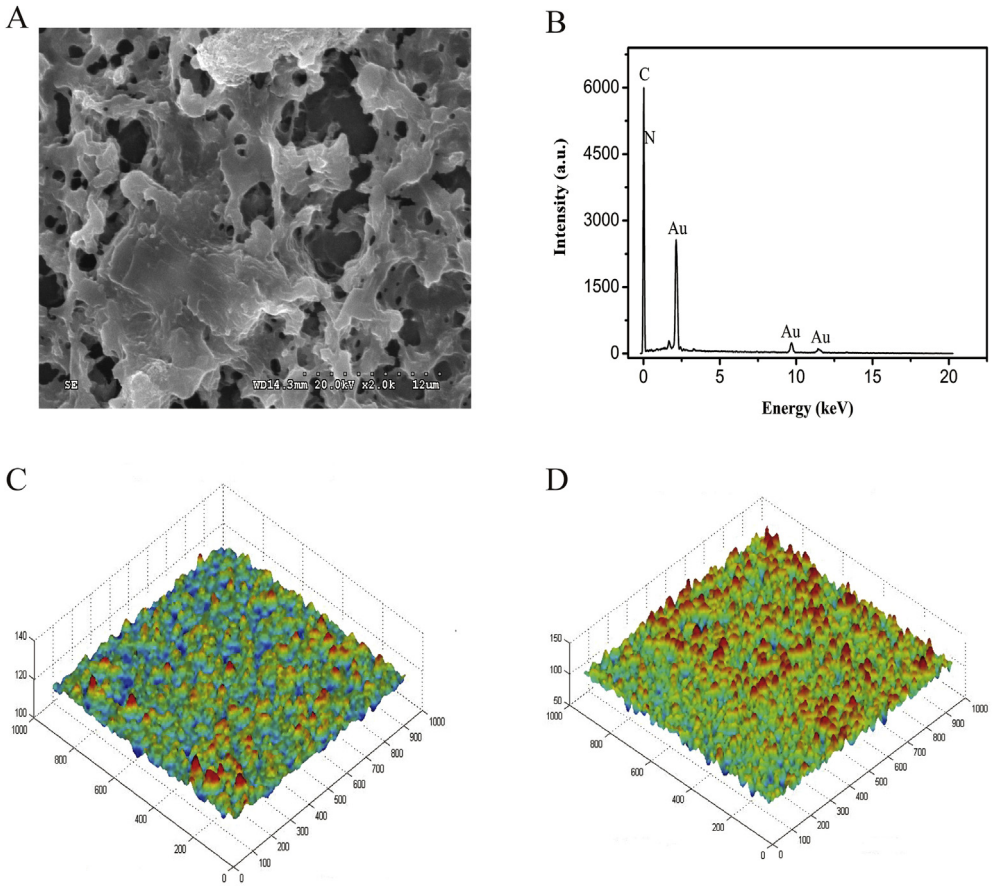

Fig. 1. (A) SEM image of prepared GS/PANI. (B) EDX spectrum of GS/PANI/AuNPs. (C) AFM image of GS/PANI/AuNPs/GCE. (D) AFM image of S/GS/PANI/AuNPs/GCE.

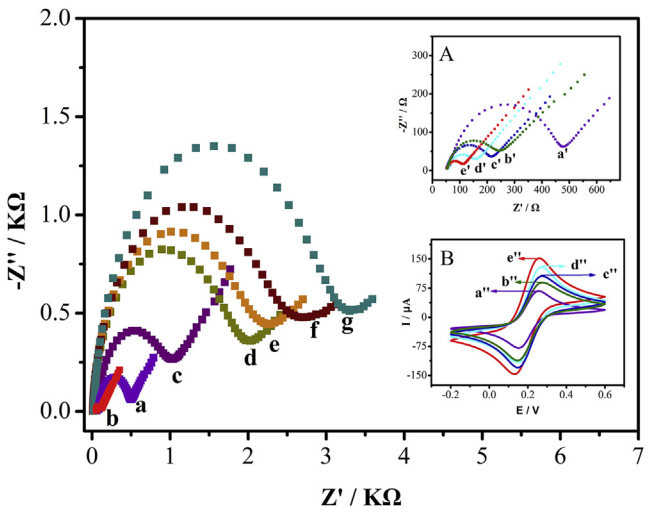

Fig. 2. EIS for each fabrication step: (a) bare GCE; (b) GS/PANI/AuNPs/GCE; (c) S/GS/PANI/AuNPs/GCE; (d) MCH/S/GS/PANI/AuNPs/GCE; (e) BSA/MCH/S/GS/PANI/AuNPs/GCE; (f) after addition of CHA reaction mixtures; (g) after attachment of SA-ALP. Inset A: EIS results of (a′) bare GCE; (b′) GS/GCE; (c′) PANI/GCE; (d′) GS/PANI/GCE; (e′) GS/PANI/AuNPs/GCE. Inset B: CV of (a″) bare GCE; (b″) GS/GCE; (c″) PANI/GCE; (d″) GS/PANI/GCE; (e″) GS/PANI/AuNPs/GCE. EIS and CV measurements were performed in 0.5 mM $Fe(CN)_6^{3-/4-}$ containing 0.4 M KCl.

background maintained increasing in the range of 60–180 min. 120 min was chosen as the optimal assembly time for CHA.

3.6. Sensitivity and specificity of the DNA biosensor

Under optimized experimental conditions, the sensitivity of this method was evaluated by DPV. Fig. 5A displayed DPV curves of the sensing system upon the addition of different concentrations of C1 (0, 10, 20, 40, 80, 160, 320, 640, 1250, 2500, 5000, 10,000, and 20,000 pM). As shown in Fig. 5B, peak current increased with concentration of C1. The peak current varied linearly with logarithm of C1 concentration in the range from 10 pM to 20 nM (Fig. 5B). The correlation coefficient (R^2) was 0.991. The detection limit was estimated to be 1.05 pM (S/N = 3). The sensing system was compared with traditional DNA biosensors based on CHA approaches and previous electrochemical biosensor toward bcr/abl (Table S2 and Table S3). Although this CHA method contained three hairpins and one single-stranded DNA which may be more costly than conventional CHA methods, it provided superior analytical performance with wider liner range and lower detection limit. Highly sensitivity of this method was attributed to two factors: (1) the GS/PANI/AuNPs could not only promote the electron transfer, but also offered effective surface area to immobilize more signal probes; (2) the DNA circuit based on toehold-mediated strand displacement, which recycled the HP:C1 duplex enabled more H1 to approach the electrode surface. In addition, the DNA circuit produced low background due to the rational design of probes sequences.

The specificity of the biosensor was evaluated using three

Please cite this article in press as: X. Chen, et al., Coupling a universal DNA circuit with graphene sheets/polyaniline/AuNPs nanocomposites for the detection of BCR/ABL fusion gene, Analytica Chimica Acta (2015), http://dx.doi.org/10.1016/j.aca.2015.06.050

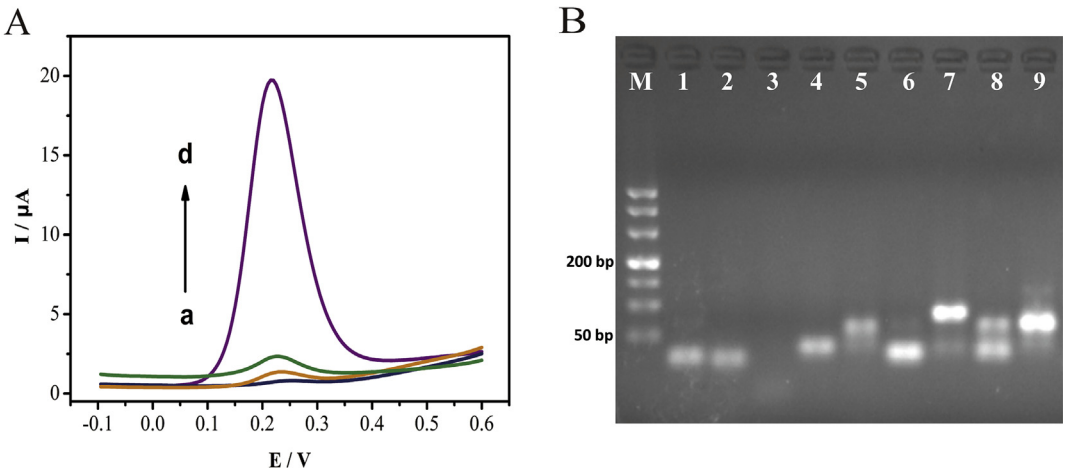

Fig. 3. (A) DPV responses of (a) 50 nM H1 + 20 nM HP, (b) 50 nM H1 + 20 nM HP + 50 nM H2, (c) 50 nM H1 + 20 nM HP + 10 nM C1, (d) 50 nM H1 + 20 nM HP + 50 nM H2 + 10 nM C1. DPV measurements were performed in DEA buffer containing 1.0 mg mL^{-1} of 1-NP. (B) The 3% agarose gel electrophoresis analysis of CHA. Different DNA samples were added into lanes 1–9. 1: H1, 2: H2, 3: C1, 4: HP, 5: C1 + HP, 6: H1 + H2, 7: C1 + HP + H1, 8: C1 + HP + H2, 9: C1 + HP + H1 + H2. The band of DL500 DNA marker from top to bottom is 500 bp, 400 bp, 300 bp, 200 bp, 150 bp, 100 bp, and 50 bp.

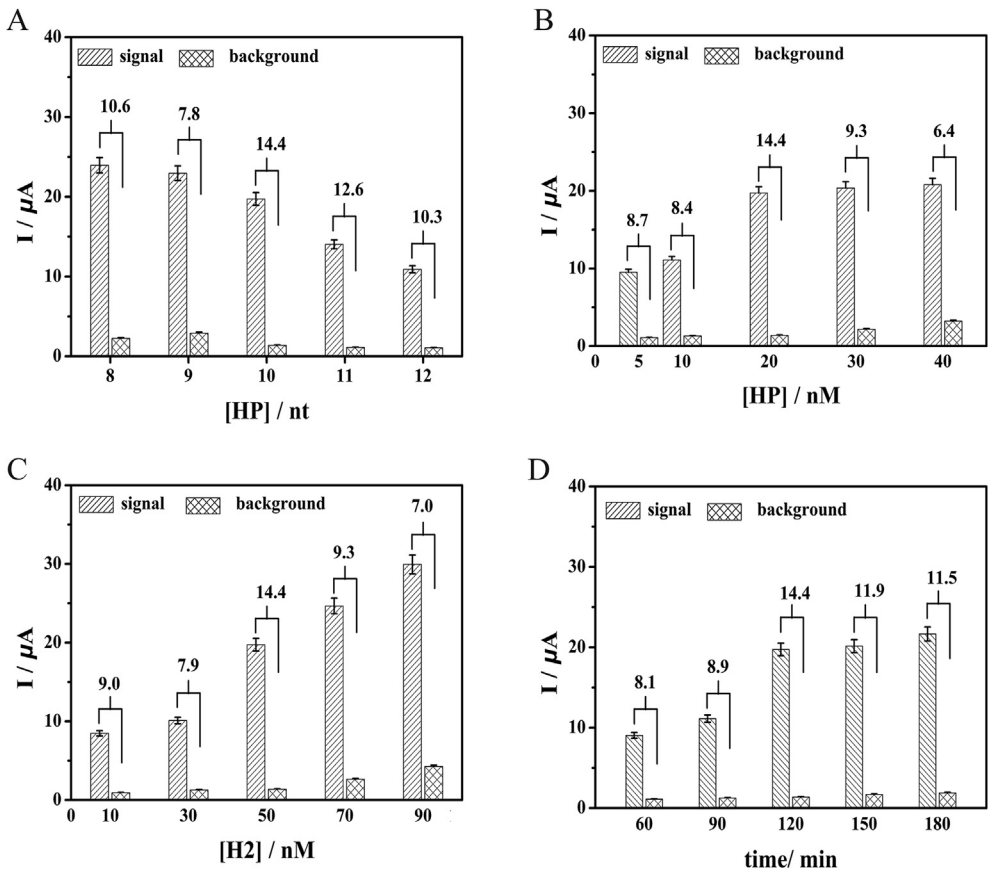

Fig. 4. Optimizations of experimental parameters: effect of (A) sequence number of HP stem; (B) concentration of HP; (C) concentration of H2; (D) assembly time for CHA. One parameter changed with the others under optimal conditions. The concentration of H1 and C1 was 50 nM and 10 nM, respectively. The numbers at the columns top was ratio of signal to background.

different DNA sequences (10 nM), including complementary target DNA, single-base mismatched, four-base mismatched and non-complementary sequence DNA. Fig. 6 showed comparison of the peak current of blank and other four DNA strands under the same conditions. The peak current of complementary target DNA was significantly higher than that of the other three DNA sequences. Moreover, the peak current of the single-base mismatched, the four-base mismatched and the non-complementary DNA were nearly as that of blank. These results demonstrated that this biosensor provided high specificity which had the potential for quantitative determination of target DNA in real samples.

Please cite this article in press as: X. Chen, et al., Coupling a universal DNA circuit with graphene sheets/polyaniline/AuNPs nanocomposites for the detection of BCR/ABL fusion gene, Analytica Chimica Acta (2015), http://dx.doi.org/10.1016/j.aca.2015.06.050

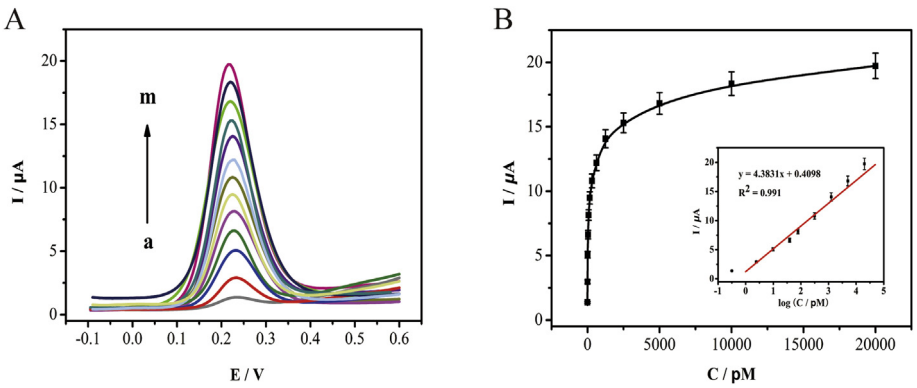

Fig. 5. (A) DPV responses for different concentrations of C1 (from a to m: 0, 10, 20, 40, 80, 160, 320, 640, 1250, 2500, 5000, 10,000, and 20,000 pM). (B) The calibration curve between the peak current and the logarithm of C1 concentration.

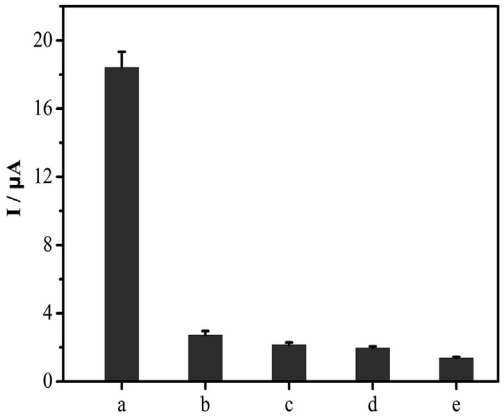

Fig. 6. Specificity of the developed method: (a) complementary DNA, (b) single-base mismatched DNA, (c) four-base mismatched DNA, (d) non-complementary DNA, (e) blank. Concentration of these DNA was 10 nM.

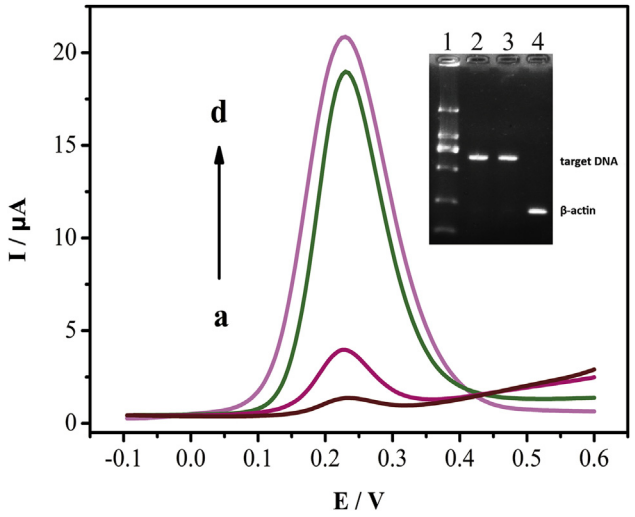

Fig. 7. DPV responses of PCR products obtained from (a) blank, (b) negative real sample, (c) K562 cells, (d) positive real sample. Inset: The 2% agarose gel electrophoresis analysis of PCR products: (lane 1) DL2000 DNA marker (the brands from top to bottom is 2000 bp, 1000 bp, 750 bp, 500 bp, 250 bp and 100 bp); (lane 2) K562 cells; (lane 3) positive real sample; (lane 4) negative real sample + β-actin.

3.7. Stability and reproducibility of the DNA biosensor

Stability of the DNA biosensor was investigated by three independent experiments. It demonstrated that the DNA biosensor could retain about 92.6% of its initial current response after two-week storage at 4 °C. Reproducibility of the biosensor was further tested. Five modified electrodes prepared with the same processes independently were used to detect target DNA (20 pM, 50 pM, and 100 pM), and the relative standard deviation was 5.26%, 4.59%, and 4.43%, respectively. Therefore, it could be concluded that the DNA biosensor provided satisfactory stability and reproducibility.

3.8. Detection of real sample

To test real application of the fabricated DNA biosensor, bcr/abl from K562 cells, positive real sample (from CML patient), and negative real sample (from normal people) were obtained by PCR amplification. The agarose gel electrophoresis of the PCR products was shown in Fig. 7 (inset). The PCR products of K562 cells and positive real sample presented the light bands at about 600 bp which were corresponded to the characteristic position of bcr/abl (lane 2 and 3), while the PCR product of negative real sample did not present any band at 600 bp (β-actin was used as loading control, lane 4). K562 cell was the mostly used cell strain of CML, which was bcr/abl positive. The band of positive real sample was consisted with that of K562 cell, indicating that the real sample was bcr/abl positive. Then PCR products were detected by the proposed method. DPV measurements for the PCR products were shown in Fig. 7. Interestingly, the fabricated biosensor performed equally well despite the fact that bcr/abl from real sample was much longer than the synthetic target DNA. This could be attributed to HP with a rationally designed loop which was able to bind longer target DNA. The DPV signals of PCR products of K562 cells and positive real sample gave a mean average of 19.21 μA and 18.45 μA (curve c and d), which were much higher than that of negative real sample and blank (curve a and b). The higher DPV signals from K562 cells and CML patient indicated their up-regulated expression of bcr/abl compared with normal people, which were consisted with the results of agarose gel electrophoresis.

4. Conclusions

In summary, we proposed a sensing strategy by employing a universal DNA circuit and GS/PANI/AuNPs for highly sensitive and specific detection of target DNA. Although this method may be a little more timing and costly than conventional CHA methods, this strategy also had several features. First, we introduced a transducer for CHA which made the DNA circuit be available for different kinds

Please cite this article in press as: X. Chen, et al., Coupling a universal DNA circuit with graphene sheets/polyaniline/AuNPs nanocomposites for the detection of BCR/ABL fusion gene, Analytica Chimica Acta (2015), http://dx.doi.org/10.1016/j.aca.2015.06.050

of targets. Second, the stem, loop, and toehold of hairpins (HP, H1, H2) were rationally designed to improve signal-to-background ratio and specificity. Third, this protocol coupled an enzyme-free DNA circuit with easily synthesized GS/PANI/AuNPs for further signal amplification. By combining advantages of CHA and GS/PANI/AuNPs, this sensing system provided high sensitivity and specificity for the detection of bcr/abl. Moreover, this biosensor was applied for the detection of real sample with satisfactory results, demonstrating its great potential in clinical application.

Acknowledgments

This work was financially supported by Natural Science Research Foundation of China (No. 81070421 to Wenli Feng, No. 81171415 to Guoming Xie) and the science & technology bureau of Yibin (2014SF015).

Appendix A. Supplementary data

Supplementary data related to this article can be found at http://dx.doi.org/10.1016/j.aca.2015.06.050.

References

[1] D.C. Tkachuk, C.A. Westbrook, M. Andreeff, T.A. Donlon, M.L. Cleary, K. Suryanarayan, M. Homge, A. Redner, J. Gray, D. Pinkel, Detection of bcr-abl fusion in chronic myelogeneous leukemia by in situ hybridization, Science 250 (1990) 559–562.
[2] A. Sharma, C.M. Pandey, G. Sumana, U. Soni, S. Sapra, A.K. Srivastava, T. Chatterjee, B.D. Malhotra, Chitosan encapsulated quantum dots platform for leukemia detection, Biosens. Bioelectron. 38 (2012) 107–113.
[3] O. Akhavan, E. Ghaderi, E. Hashemi, R. Rahighi, Ultra-sensitive detection of leukemia by graphene, Nanoscale 6 (2014) 14810–14819.
[4] H.G. Goh, M. Lin, T. Fukushima, G. Saglio, D. Kim, S.Y. Choi, S.H. Kim, J. Lee, Y.S. Lee, S.M. Oh, Sensitive quantitation of minimal residual disease in chronic myeloid leukemia using nanofluidic digital polymerase chain reaction assay, Leuk. Lymphoma 52 (2011) 896–904.
[5] M. Labib, S.M. Ghobadloo, N. Khan, D.M. Kolpashchikov, M.V. Berezovski, Four-way junction formation promoting ultrasensitive electrochemical detection of microRNA, Anal. Chem. 85 (2013) 9422–9427.
[6] J. Hu, Y. Yu, J.C. Brooks, L.A. Godwin, S. Somasundaram, F. Torabinejad, J. Kim, C. Shannon, C.J. Easley, A reusable electrochemical proximity assay for highly selective, real-time protein quantitation in biological matrices, J. Am. Chem. Soc. 136 (2014) 8467–8474.
[7] M.U. Kopp, A.J. Mello, A. Manz, Chemical amplification: continuous-flow PCR on a chip, Science 280 (1998) 1046–1048.
[8] Q. Xue, Y. Lv, H. Cui, X. Gu, S. Zhang, J. Liu, A DNA nanomachine based on rolling circle amplification-bridged two-stage exonuclease III-assisted recycling strategy for label-free multi-amplified biosensing of nucleic acid, Anal. Chim. Acta 856 (2015) 103–109.
[9] Y. Hu, X. Xu, Q. Liu, L. Wang, Z. Lin, G. Chen, Ultrasensitive electrochemical biosensor for detection of DNA from bacillus subtilis by coupling target-induced strand displacement and nicking endonuclease signal amplification, Anal. Chem. 86 (2014) 8785–8790.
[10] Q. Guo, Y. Chen, Z. Song, L. Guo, F. Fu, G. Chen, Label-free and enzyme-free sensitive fluorescent detection of human immunodeficiency virus deoxyribonucleic acid based on hybridization chain reaction, Anal. Chim. Acta 852 (2014) 244–249.
[11] Y. Jiang, B. Li, J.N. Milligan, S. Bhadra, A.D. Ellington, Real-time detection of isothermal amplification reactions with thermostable catalytic hairpin assembly, J. Am. Chem. Soc. 135 (2013) 7430–7433.
[12] Y. Qian, D. Tang, L. Du, Y. Zhang, L. Zhang, F. Gao, A novel signal-on electrochemical DNA sensor based on target catalyzed hairpin assembly strategy, Biosens. Bioelectron. 64 (2015) 177–181.
[13] Y. Qian, C. Wang, F. Gao, Assistant deoxyribonucleic acid recycling with Zn^{2+} and molecular beacon for electrochemical detection of deoxyribonucleic acid via target-triggered assembly of mutated DNAzyme, Anal. Chim. Acta. 845 (2014) 1–6.
[14] P. Yin, H.M. Choi, C.R. Calvert, N.A. Pierce, Programming biomolecular self-assembly pathways, Nature 451 (2008) 318–322.
[15] D.Y. Zhang, A.J. Turberfield, B. Yurke, E. Winfree, Engineering entropy-driven reactions and networks catalyzed by DNA, Science 318 (2007) 1121–1125.
[16] D.Y. Zhang, G. Seelig, Dynamic DNA nanotechnology using strand-displacement reactions, Nat. Chem. 3 (2011) 103–113.
[17] B. Zhang, B. Liu, D. Tang, R. Niessner, G. Chen, D. Knopp, DNA-based hybridization chain reaction for amplified bioelectronic signal and ultrasensitive detection of proteins, Anal. Chem. 84 (2012) 5392–5399.
[18] Y. Qian, D. Tang, L. Du, Y. Zhang, L. Zhang, F. Gao, A novel signal-on electrochemical DNA sensor based on target catalyzed hairpin assembly strategy, Biosens. Bioelectron. 64 (2015) 177–181.
[19] B.C. Yin, Y.M. Guan, B.C. Ye, An ultrasensitive electrochemical DNA sensor based on the ssDNA-assisted cascade of hybridization reaction, Chem. Commun. 48 (2012) 4208–4210.
[20] Y.S. Jiang, S. Bhadra, B. Li, A.D. Ellington, Mismatches improve the performance of strand displacement nucleic acid circuits, Angew. Chem. Int. Ed. 126 (2014) 1876–1879.
[21] J. Chen, J. Zhang, K. Wang, L. Huang, X. Lin, G. Chen, Electrochemical biosensor based on hairpin DNA probe using 2-nitroacridone as electrochemical indicator for detection of DNA species related to chronic myelogenous leukemia, Electrochem. Commu 10 (2008) 1448–1451.
[22] L. Lin, J. Chen, Q. Lin, W. Chen, J. Chen, H. Yao, A. Liu, X. Lin, Y. Chen, Electrochemical biosensor based on nanogold-modified poly-eriochrome black T film for BCR/ABL fusion gene assay by using hairpin LNA probe, Talanta 80 (2010) 2113–2119.
[23] L. Hu, T. Tan, G. Chen, K. Zhang, J.J. Zhu, Ultrasensitive electrochemical detection of BCR/ABL fusion gene fragment based on polymerase assisted multiplication coupling with quantum dot tagging, Electrochem. Commu 35 (2013) 104–107.
[24] G. Aragay, F. Pino, A. MerkoÇi, Nanomaterials for sensing and destroying pesticides, Chem. Rev. 112 (2012) 5317–5338.
[25] A. Ambrosi, C.K. Chua, A. Bonanni, M. Pumera, Electrochemistry of graphene and related materials, Chem. Rev. 114 (2014) 7150–7188.
[26] J. Pecher, S. Mecking, Nanoparticles of conjugated polymers, Chem. Rev. 110 (2010) 6260–6279.
[27] S. Samanman, A. Numnuam, W. Limbut, P. Kanatharana, P. Thavarungkul, Highly-sensitive label-free electrochemical carcinoembryonic antigen immunosensor based on a novel Au nanoparticles-graphene-chitosan nanocomposite cryogel electrode, Anal. Chim. Acta 853 (2015) 521–532.
[28] J.N. Zadeh, C.D. Steenberg, J.S. Bois, B.R. Wolfe, M.B. Pierce, A.,R. Khan, R.M. Dirks, N.A. Pierce, NUPACK: analysis and design of nucleic acid systems, J. Comput. Chem. 32 (2011) 170–173.
[29] F.Y. Kong, S.X. Gu, W.W. Li, T.T. Chen, Q. Xu, W. Wang, A paper disk equipped with graphene/polyaniline/Au nanoparticles/glucose oxidase biocomposite modified screen-printed electrode: toward whole blood glucose determination, Biosens. Bioelectron. 56 (2014) 77–82.
[30] C. Song, G. Xie, L. Wang, L. Liu, G. Tian, H. Xiang, DNA-based hybridization chain reaction for an ultrasensitive cancer marker EBNA-1 electrochemical immunosensor, Biosens. Bioelectron. 58 (2014) 68–74.
[31] D.Y. Zhang, E. Winfree, Control of DNA strand displacement kinetics using toehold exchange, J. Am. Chem. Soc. 131 (2009) 17303–17314.
[32] L. Wang, E. Hua, M. Liang, C. Ma, Z. Liu, S. Sheng, M. Liu, G. Xie, W. Feng, Graphene sheets, polyaniline and AuNPs based DNA sensor for electrochemical determination of BCR/ABL fusion gene with functional hairpin probe, Biosens. Bioelectron. 51 (2014) 201–207.
[33] B. Li, A.D. Ellington, X. Chen, Rational, modular adaptation of enzyme-free DNA circuits to multiple detection methods, Nucleic Acids Res. 39 (2011) e110.
[34] Z. Peng, L. Guo, Z. Zhang, B. Tesche, T. Wilke, D. Ogermann, S. Hu, K. Kleinermanns, Micelle-assisted one-pot synthesis of water-soluble polyaniline-gold composite particles, Langmuir 22 (2006) 10915–10918.
[35] J. Han, J. Ma, Z. Ma, One-step synthesis of graphene oxide-thionine-Au nanocomposites and its application for electrochemical immunosensing, Biosens. Bioelectron. 47 (2013) 243–247.

Please cite this article in press as: X. Chen, et al., Coupling a universal DNA circuit with graphene sheets/polyaniline/AuNPs nanocomposites for the detection of BCR/ABL fusion gene, Analytica Chimica Acta (2015), http://dx.doi.org/10.1016/j.aca.2015.06.050